Computational and Theoretical Chemistry 1207 (2022) 113487

Contents lists available at ScienceDirect

Computational and Theoretical Chemistry

journal homepage: www.elsevier.com/locate/comptc

The molecular mechanism of electroporation: Changes in the hydrogen bonds

Ming-hui Ji [a], Jia-hao Xu [a], Sha-sha Yuan [a], Ya-wen Liu [a], Xin-yi Xing [a], Chao Jiang [a,*], Liang Xue [a,*], Chuan-kai Yang [b], Feng-hong Chu [a], You-hua Jiang [a]

[a] College of Electronics and Information Engineering, Shanghai University of Electric Power, Shanghai 200090, China
[b] State Grid Shaanxi Electric Power Research Institute, Hangtian Mid RD.669, Changan Dist, Xi'an, Shaanxi, China

ARTICLE INFO

Keywords:
Electroporation
Membrane
Electric field
Molecular dynamics
Quantum chemistry

ABSTRACT

Electroporation has many technological applications in drug delivery and gene transfection. However, the molecular mechanism of electroporation is unknown. Thus, we propose for the first time that hydrogen bonds play a key role during electroporation based on molecular dynamics and quantum chemistry methods. The electric field affects the hydrogen-bonded network in the membrane system, which induces water molecules to pass through the membrane. Our findings reveal the mechanism of electroporation in atomic details and may have a potential application in controlling the permeability of cell membranes.

1. Introduction

The permeability of a cell membrane can be transiently increased by applying external electric field pulses [1]. It provides a non-chemical approach to the delivery of molecules across the cell membrane and has many promising medical applications [2]. However, the molecular mechanism of electroporation is currently unclear. Many explanations have been offered for the phenomenon. One of the most convincing explanations for the mechanism is water pore formation model [3]. According to Tieleman's investigation, pore formation was promoted by an increased likelihood of transmembrane water defects in the presence of an external electric field. And water defects were caused by the interaction of water dipoles with the electric field gradient at the water/lipid or water/octane interface [4]. Tokman, using molecular dynamics simulations, demonstrated that pore formation is driven by the reorganization of the interfacial water molecules [5]. Bing Bu showed that the electric field inside the membrane became heterogeneous under the applied electric field. This hetero- generous electric field reorientated the dipole direction of water molecules in a direction antiparallel to that of the electric field and then imposed unbalanced electric forces on the water molecules, which drove the water molecules into the membrane [6]. Cheng Zhou simulated the electroporation process caused by the uneven ion distribution and divided the process into three stages: pore formation stage, pore maintenance stage and pore healing stage [7]. From the perspective of hydrogen bonds, Tieleman found that pore formation is enthalpically favorable in a DMPC bilayer, and the free energy cost was due to a large unfavorable entropy. The total number of hydrogen bonds in the system was maintained during pore formation, although the number of water-water hydrogen bonds decreased at the expense of increased lipid-water hydrogen bonds [8].

In this work, we use the method of molecular dynamics simulation to study the molecular mechanism of electroporation. Quantum chemistry methods are used to calculate the strength of hydrogen bonds. This study provides a theoretical basis for electroporation technology.

2. Simulation methods

2.1. Preparation of models and molecular dynamics simulations

Lipid bilayers were generated by the CHARMM-GUI online service [9]. The phospholipid membrane was composed of 1,2-dipalmitoyl-*sn*-*glycero*-3-phospho choline (DPPC). The whole system is mainly composed of 200 lipid molecules, 7569 water molecules of the OPC4 water model [10], and contains 19 Cl− and 19 K+ distributing on both sides of the membrane evenly (corresponding to a physiological concentration of 0.15 M). Simulations and analyses of the electroporation process were performed using the GROMACS package [11] with CHARMM36 force field [12]. A periodic boundary condition was applied. The temperature was coupled to 323 K with the V-rescale algorithm [13] and the coupling constants were 1.0 ps. The pressure was

* Corresponding authors.
E-mail addresses: jiangchao@shiep.edu.cn (C. Jiang), xueliangokay@gmail.com (L. Xue).

https://doi.org/10.1016/j.comptc.2021.113487
Received 27 August 2021; Received in revised form 5 October 2021; Accepted 18 October 2021
Available online 27 October 2021

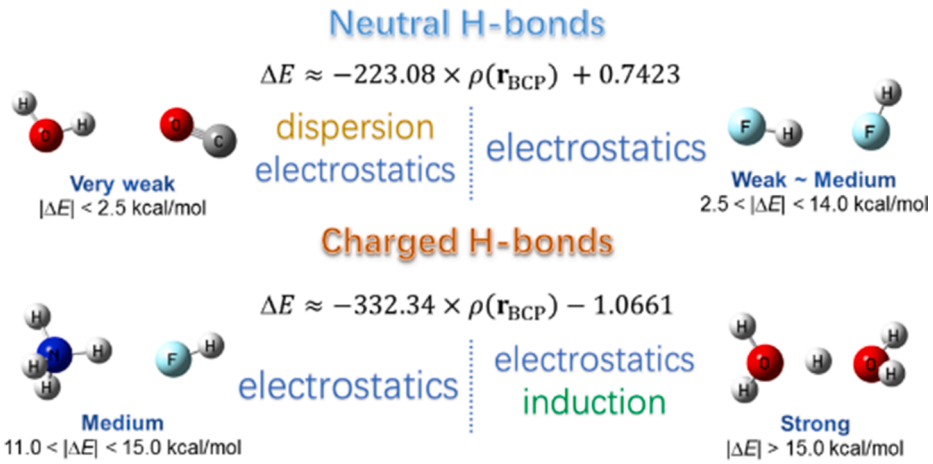

Fig. 1. Methods of estimating the strength of hydrogen bonds.

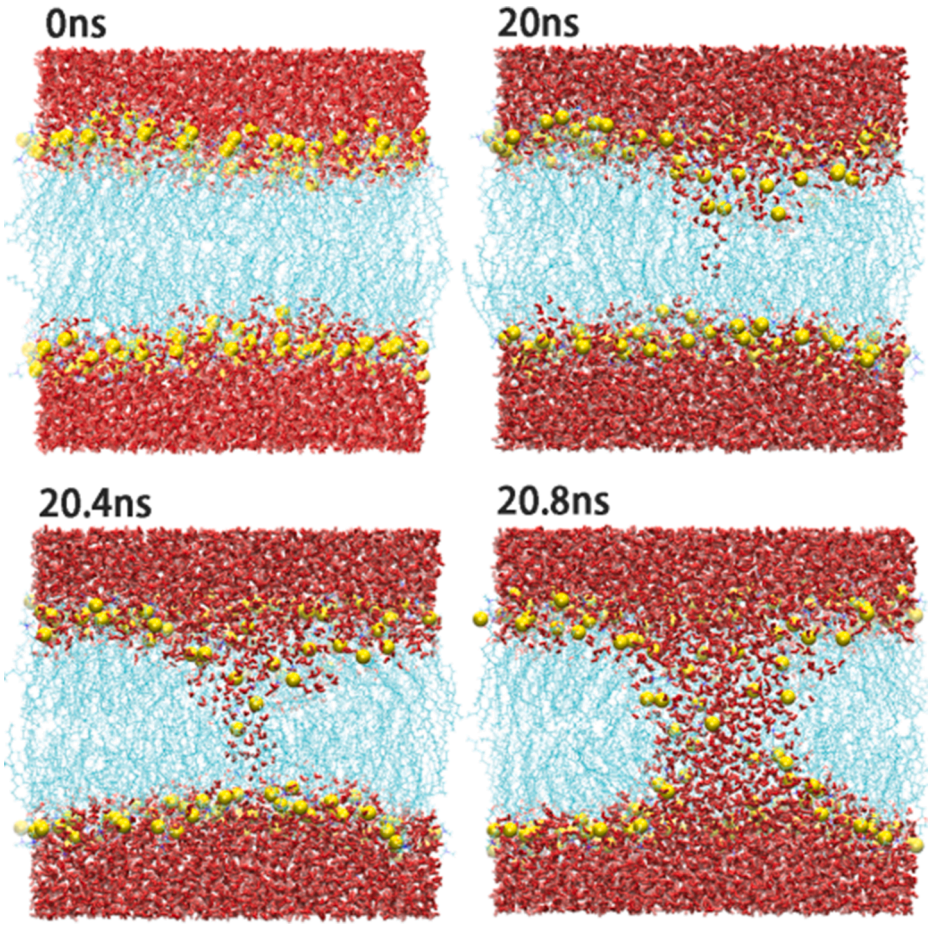

Fig. 2. The process of the electroporation. The red represents water molecules. The blue represents phospholipid molecules. The yellow sphere represents the phosphorus atoms.

coupled to 1 bar using the Berendsen method [14] and the coupling constants were 4.0 ps. The LINCS algorithm[15] was applied to constrain the covalent bonds with H-atoms. The time step was 2.0 fs. The Lennard-Jones effect was truncated at 1.2 nm and translated from 0.9 nm to 1.2 nm. The particle mesh Ewald (PME) method was used [16] with a cutoff radius of 1.2 nm. The electric field intensity is set to a 0.5v/nm pulsed electric field. Electroporation process and electrostatic interaction analyses were shown by the VMD [17].

2.2. Quantum chemical simulations

We cut a cluster containing phospholipid molecules and water molecules in the original structure and replaced the hydrophobic part of the phospholipid molecules with methyl groups to save calculations. The structure contained 8 water molecules and 3 phospholipid molecules with a total of 162 atoms. Three phospholipid molecules once formed hydrogen bonds with water filaments. Within a distance cutoff of 2 Å, 8 water molecules contacted closely with 3 phospholipid molecules. The

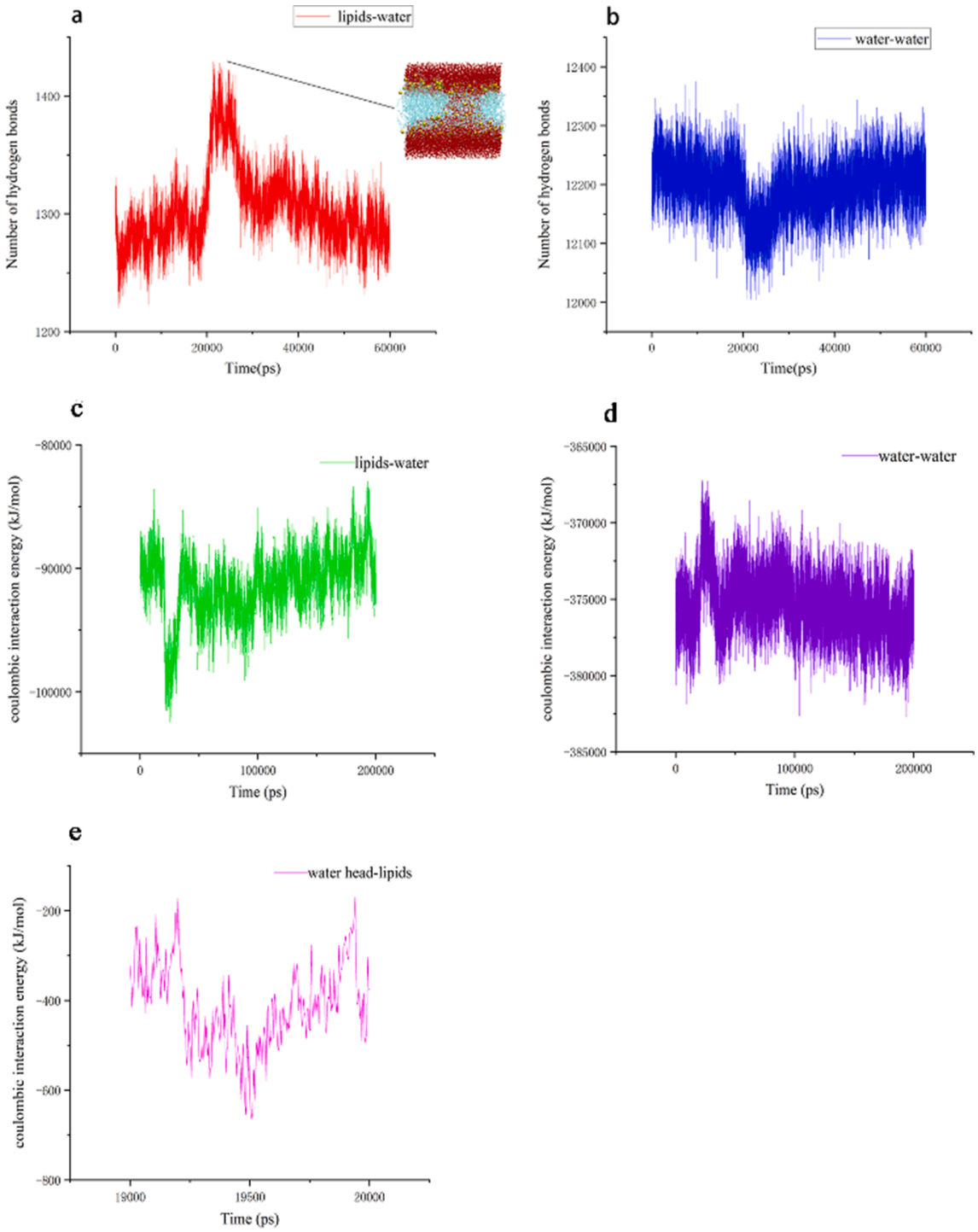

Fig. 3. (a-b) The number of hydrogen bonds. The red represents the hydrogen bonds between lipids and water. The blue represents the hydrogen bonds in the water molecules. (c-d) The electrostatic interaction energy. The 'water-head' molecules represent the water molecules that first move to the opposite side of the membrane to form water filament.

hydrogen bonds formed by water molecules in close contact with phospholipids had a higher hydrogen bond strength than other water molecules that are farther away. The quantum chemical calculations were performed in the ORCA 4.2.1 package [18]. Full DFT optimization (with default optimization criteria) of the structure used the B97-3c composite scheme [19]. The single point energies of the cluster were calculated at the wB97M-V/def2-TZVP level [20,21]. The electron density of the bond critical point (BCP) was used to calculate the hydrogen bond binding energy to estimate the hydrogen bond strength [22] as seen in Fig. 1. To understand the weak interaction between water molecules and phospholipid molecules, the IGMH (IGM [23] based on Hirshfeld partition of molecular density) implemented on the Multiwfn 3.8 program [24] was carried out for the cluster.

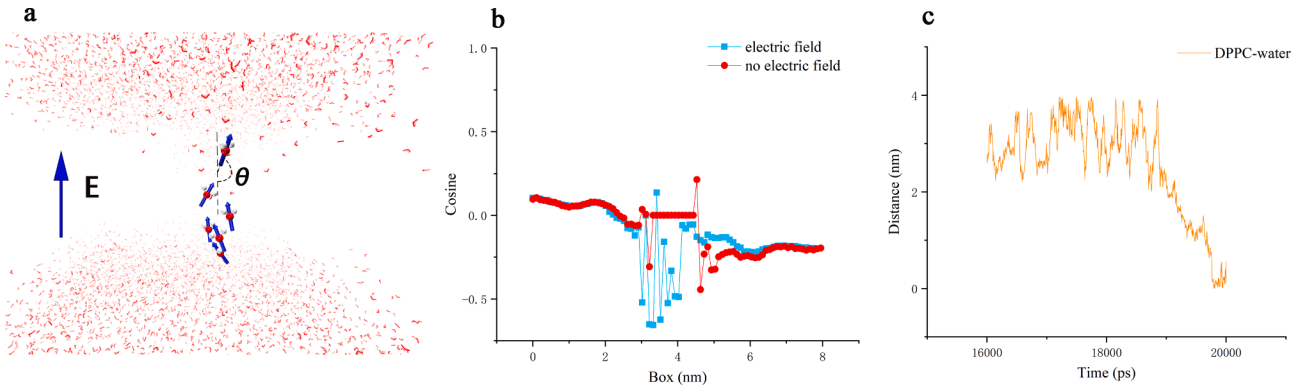

Fig. 4. (a) The blue arrows represent the dipole moment of water molecules. The θ represents the angle between the water dipole moment and the box normal (b) The distribution of cos(θ) in the normal direction (z direction) of the box. (c) The distance between the water-head molecules and the phospholipid molecules.

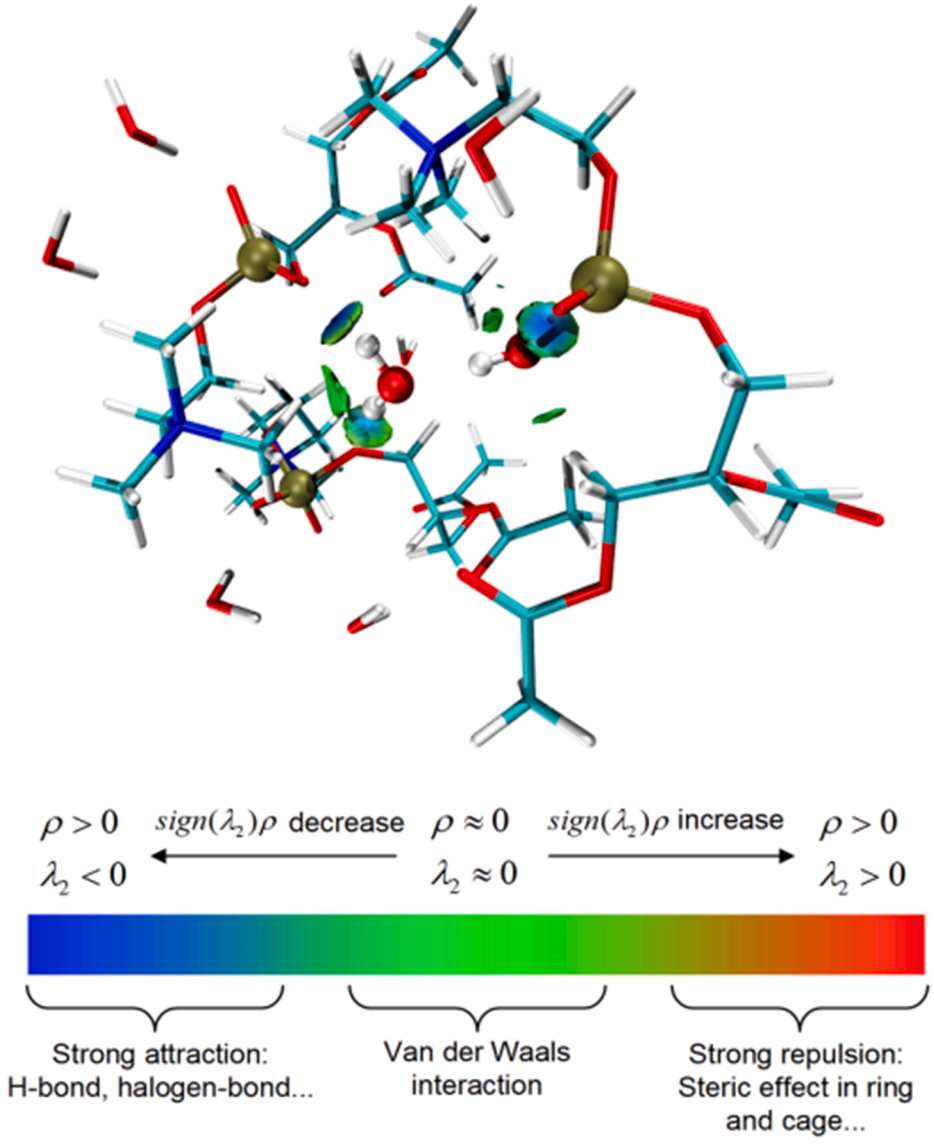

Fig. 5. IGMH analysis. The blue represents hydrogen bonding. The green represents van der Waals interaction.

3. Results and disscussion

3.1. Membrane perforation process

The maximum intensity of the pulsed electric field is set to 0.5v/nm. The pulse starts at 16.712 ns and reaches its peak at 20 ns. According to the multiple simulation tests, this kind of electric field can easily cause perforation. As shown in Fig. 2, water filaments begin to form at 20 ns and water chains start to form at 20.4 ns. Only 0.4 ns later, a water column appears. It can be seen from the trajectory that part of the water molecules break away from the hydrophilic area of the phospholipid and reach the hydrophobic area to meet with the water molecules on the opposite side. We shall call it the process of formatting the water filament. Other water molecules follow the water filament to form a water column. The hydrophilic area of phospholipid molecules is also driven by the water column to form a hydrophilic pathway.

3.2. The hydrogen bonds and interaction energy

As can be observed in Fig. 3. a-b, the number of hydrogen bonds shows opposite trends in different hydrogen-bonded networks at 20 ns. It indicates that some water molecules will escape from the stable water system and enter the interior of the phospholipid molecules to form new hydrogen bonds. In detail, the number of hydrogen bonds in the water molecules starts to decrease at 17.5 ns, which proves that the electric field will destroy the hydrogen-bonded network in the original stable water subsystem at the beginning of electroporation. These escaped water molecules reach the hydrophilic area of the phospholipids and begin to form additional hydrogen bonds with the phospholipid molecules at 18 ns. The increase in the number of hydrogen bonds corresponds to the increase in electrostatic interaction energy, which can also reflect the dynamic process of water molecules as shown in Fig. 3. c-d.

In order to reflect the details of the formation of the water filament, we have investigated the changes in the coulombic interaction energy between phospholipid molecules and water molecules in the water filaments (water-head molecules). The interaction energy between the water-head molecules and the hydrophilic area of phospholipid molecules is 322.6 kJ/mol at 19 ns. The energy increases to 609.68 kJ/mol at 19.5 ns. Only 0.5 ns later, the energy reduces to 375.6 kJ/mol. It indicates that the water molecules first form hydrogen bonds with the hydrophilic region of phospholipid molecules, then get rid of the restriction of the hydrogen bonds to reach the hydrophobic region and contact the water molecules on the other side of the membrane to form water filaments in the membrane.

3.3. Dynamic behavior of water molecules

The changes of dipole moment are an important factor influencing the hydrogen-bonded network in the water subsystem. The direction of water dipole moment tends to the direction of the electric field as can be observed in the changes of θ, which is more than $150^{\circ}(\cos(\theta) < -0.5)$ when under the electric field as seen in Fig. 4. a-b. In fact, the trend of rotation is not conducive to the formation of the hydrogen-bonded network and gives water molecules more chances to escape from the network. Changes in the distance between the water-head molecules and phospholipids indicate that water-head molecules leave the water system and enter the hydrophilic area of phospholipids at 19 ns, before the formation of water filaments. These water-head molecules will cause the hydrophilic area of phospholipid molecules to become very crowded. In fact, the hydrophilic area of phospholipid molecules can only form hydrogen bonds with a limited number of water molecules. Crowded water molecules with the rotation trend of water dipole moment would cause the hydrogen bonds to become much weaker. As introduced in Section 3.4, this kind of the hydrogen bonds inherently are very weak under normal conditions. The phospholipid molecules would not bind the water molecules tightly under the circumstances, causing them to move to the hydrophobic area to meet with the water molecules on the other side.

3.4. Weak interaction analysis

Water molecules only form hydrogen bonds with the phosphate groups in the hydrophilic region of the phospholipid molecules and form van der Waals interactions with other head groups as shown in Fig. 5. The intensity of the hydrogen bonds estimated from the electron density is approximately 5.23 kcal/mol, which is a kind of weak hydrogen bonds as shown in Fig. 1.[22] This indicates that the combination of water molecules and the hydrophilic area will be easily disturbed by the external environment.

4. Conclusions

In this study, we demonstrated that hydrogen bonds play a key role during the process of electroporation for the first time. Hydrogen bonds within water molecules or between water molecules and phospholipid molecules keep the entire system stable under normal circumstances. But when under an external electric field, the hydrogen-bonded network of water subsystem would be destroyed. In order to seek a more stable binding environment, a large number of water molecules move to the hydrophilic area of phospholipids and form hydrogen bonds with them. However, the hydrogen bonds with the phosphate groups are weak. The thermal motion of water molecules and the rotation effect of external electric field cause these hydrogen bonds to be unstable. The water molecules would easily escape from the hydrophilic area, and then pass through the hydrophobic area to combine with the water molecules on the other side. Interestingly, as more and more water molecules pass through the lipid bilayer to form a water column, the lipid head group is also drawn by the water column to form a hydrophilic channel. Our findings may help control the permeability of cell membranes in drug delivery and gene transfection.

CRediT authorship contribution statement

Ming-hui Ji: Software, Validation, Investigation, Writing – original draft. **Jia-hao Xu:** Writing – review & editing. **Sha-sha Yuan:** Data curation. **Ya-wen Liu:** Visualization. **Xin-yi Xing:** Writing – review & editing. **Chao Jiang:** Writing – review & editing, Supervision. **Liang Xue:** Methodology, Data curation, Writing – review & editing, Supervision. **Chuan-kai Yang:** Writing – review & editing. **Feng-hong Chu:** Writing – review & editing. **You-hua Jiang:** Writing – review & editing.

Declaration of Competing Interest

The authors declare that they have no known competing financial interests or personal relationships that could have appeared to influence the work reported in this paper.

Acknowledgments

This work was supported by National Natural Science Foundation of China (62105196) and Shanghai Sailing Program (17YF1407000).

Appendix A. Supplementary material

Supplementary data to this article can be found online at https://doi.org/10.1016/j.comptc.2021.113487.

References

[1] J.C. Weaver, Y.A. Chizmadzhev, Theory of electroporation: a review, Bioelectrochem. Bioenerg. 41 (2) (1996) 135–160.
[2] C. Chen, S.W. Smye, M.P. Robinson, J.A. Evans, Membrane electroporation theories: a review, Med. Bio Eng. Comput. 44 (1-2) (2006) 5–14.

[3] A. Yadollahpour, Z. Rezaee, Electroporation as a New Cancer Treatment Technique: A Review on the Mechanisms of Action, Biomed. Pharmacol. J. 7 (1) (2014) 53–62.
[4] D.P. Tieleman, The molecular basis of electroporation, BMC Biochem. 5 (1) (2004) 10.
[5] M. Tokman, J.H. Lee, Z.A. Levine, M.-C. Ho, M.E. Colvin, P.T. Vernier, J. M. Sanchez-Ruiz, Electric field-driven water dipoles: nanoscale architecture of electroporation, PLoS ONE 8 (4) (2013) e61111.
[6] B. Bu et al., Mechanics of water pore formation in lipid membrane under electric field. Springer, 2017, 2.
[7] C. Zhou, Molecular dynamics simulation of reversible electroporation with Martini force feld, BioMed. Eng. OnLine 18 (123) (2019).
[8] W.F.D. Bennett, N. Sapay, D.P. Tieleman, Atomistic Simulations of Pore Formation and Closure in Lipid Bilayers, Biophys. J. 106 (1) (2014) 210–219.
[9] S. Jo, T. Kim, V.G. Iyer, W. Im, J. Comput. Chem. 29 (2008) 1859–1865.
[10] S. Izadi, R. Anandakrishnan, A.V. Onufriev, Building Water Models: A Different Approach, J. Phys. Chem. Lett. 5 (2014) 3863–3871.
[11] M.J. Abraham, T. Murtola, R. Schulz, S. Páll, J.C. Smith, B. Hess, E. Lindahl, GROMACS: high performance molecular simulations through multi-level parallelism from laptops to supercomputers, SoftwareX 1-2 (2015) 19–25.
[12] R.W. Pastor, A.D. MacKerell, Development of the CHARMM Force Field for Lipids, J. Phys. Chem. Lett. 2 (13) (2011) 1526–1532.
[13] G. Bussi, D. Donadio, M. Parrinello, Canonical sampling through velocity rescaling, J. Chem. Phys. 126 (1) (2007) 014101, https://doi.org/10.1063/1.2408420.
[14] H.J.C. Berendsen, J.P.M. Postma, W.F. van Gunsteren, A. DiNola, J.R. Haak, Molecular dynamics with coupling to an external bath, J. Chem. Phys. 81 (8) (1984) 3684–3690.
[15] B. Hess, P-LINCS: a parallel linear constraint solver for molecular simulation, J. Chem. Theory Comput. 4 (2008) 116–122.
[16] U. Essmann, L. Perera, M.L. Berkowitz, T. Darden, H. Lee, L.G. Pedersen, A smooth particle mesh Ewald method, J. Chem. Phys. 103 (19) (1995) 8577–8593.
[17] W. Humphrey, A. Dalke, K. Schulten, VMD: Visual molecular dynamics, J. Mol. Graph. 14 (1) (1996) 33–38.
[18] F. Neese, Wiley Interdiscip. Rev. Comput. Mol. Sci. 2 (2012) 73–78.
[19] J.G. Brandenburg, C. Bannwarth, A. Hansen, S. Grimme, B97–3c: a revised low-cost variant of the B97-D density functional method, J. Chem. Phys. 148 (6) (2018) 064104, https://doi.org/10.1063/1.5012601.
[20] N. Mardirossian, M. Head-Gordon, ωB97M-V: A combinatorially optimized, range-separated hybrid, meta-GGA density functional with VV10 nonlocal correlation, J. Chem. Phys. 144 (21) (2016) 214110, https://doi.org/10.1063/1.4952647.
[21] A. Schafer, C. Huber, R. Ahlrichs, J. Chem. Phys. 100 (1994) 5829–5835.
[22] S. Emamian, T. Lu, H. Kruse, H. Emamian, J. Comput. Chem. 40 (2019) 2868.
[23] C. Lefebvre, G. Rubez, H. Khartabil, J.-C. Boisson, J. Contreras-García, E. Hénon, PCCP 19 (2017) 17928–17936.
[24] T. Lu, F. Chen, J. Comput. Chem. 33 (2012) 580–592.